

THE NUCLEAR AND EXTENDED INFRARED EMISSION OF THE SEYFERT GALAXY NGC 2992 AND THE INTERACTING SYSTEM Arp 245

Ismael García-Bernet^{1,2}, Cristina Ramos Almeida^{1,2}, Jose Acosta-Pulido^{1,2}, et al.



¹ Instituto de Astrofísica de Canarias, Calle Vía Láctea, s/n, La Laguna, Tenerife, Spain
² Departamento de Astrofísica, Universidad de La Laguna, La Laguna, Tenerife, Spain



ULL
 Universidad
 de La Laguna

ABSTRACT

We present subarcsecond resolution infrared (IR) imaging and mid-IR (MIR) spectroscopic observations of the Seyfert 1.9 galaxy NGC 2992. The data were obtained using the Gran Telescopio CANARIAS (GTC). In the N-band, the galaxy was observed with a spatial resolution of $0.32''$ (55 pc) and the imaging data reveal extended faint emission out to about 3 kpc, with a surface brightness of 4.8 mJy/arcsec². By comparing the MIR spectra of the nuclear and extended emission of the galaxy, we conclude that the origin of the extended emission is likely dust in the inner galaxy disk, with some contribution from star formation. We also report arcsecond resolution MIR and far-IR (FIR) imaging of the interacting system Arp 245 (NGC 2992, NGC 2993 and Arp 245 North), taken with the Spitzer Space Telescope and the Herschel Space Observatory. For NGC 2992, we obtained Spitzer MIR and Herschel FIR nuclear fluxes using different methods and compared them with the subarcsecond resolution data. Using imaging data, we find that we can only recover the nuclear fluxes obtained from high angular resolution data at 20 – 25 μ m, where emission from the AGN dominates. We fitted the nuclear IR spectral energy distribution (SED) of NGC 2992, including the 7.5 – 13 μ m GTC/CanariCam (CC) nuclear spectrum, with clumpy torus models. We then used the best-fitting torus model to decompose the 5 – 30 μ m Spitzer/IRS spectrum (~ 630 pc) in AGN and starburst (SB) components, using different SB templates. We find that, whereas at shorter wavelengths the SB component dominates the MIR emission, with 64% contribution at 6 μ m, the AGN component reaches 90% at 20 μ m. Finally, we reproduced the dust emission of the Arp 245 system using a set of modified blackbodies, from which we derived dust temperatures, star formation rates (SFRs) and dust masses.

High angular resolution images of NGC 2992.

We present high angular resolution MIR images obtained with MICHELLE, on the GN (see Fig. 1) and optical and near-IR (NIR) from the Hubble Space Telescope (HST; see Fig. 2). The N-band image reveals faint extended emission along PA $\sim 30^\circ$ and extending out to ~ 3 kpc. This is coincident with the extended emission shown in the NIR HST image and it is elongated in the same direction as the dust lane detected in the optical HST image (see Fig. 2).

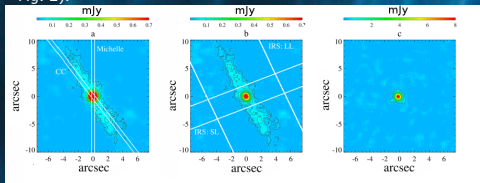


Fig. 1.- GN/MICHELLE images of NGC 2992. (a) MICHELLE 11.2 μ m image, (b) PSF-subtracted MICHELLE 11.2 μ m image at 90% level and (c) MICHELLE 18.1 μ m image. All images are smoothed. North is up, and east to the left.

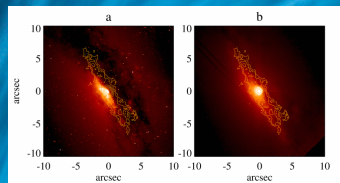


Fig. 2.- (a) HST/WFPC2 optical image of NGC 2992 in the F606W filter. (b) HST/NICMOS NIR image in the F205W filter. Orange contours are those from Fig. 1b. North is up, and east to the left.

Nuclear SED modelling with clumpy torus models.

We used the Bayesian tool *Bayesclumpy*¹ to fit the nuclear IR SED of NGC 2992 and derive its torus properties.

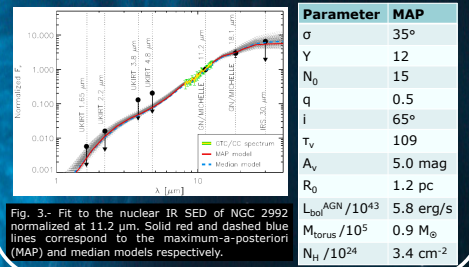


Fig. 3.- Fit to the nuclear IR SED of NGC 2992 normalized at 11.2 μ m. Solid red and dashed blue lines correspond to the maximum-a-posteriori (MAP) and median models respectively.

High angular resolution spectroscopy.

We present high angular resolution nuclear spectra of NGC 2992, which do not show PAH features and they exhibit [S IV] 10.5 μ m emission (AGN tracer). As opposed, the Spitzer/IRS spectrum shows PAH bands, indicative of the presence of SF on the scales probed by Spitzer.

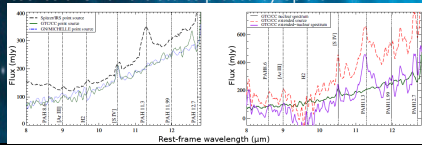


Fig. 4.- Left panel: Spitzer/IRS spectrum (dashed black line) and high angular resolution spectra (in colour) extracted as a point source. Right panel: GTC/CC spectrum of the nucleus extracted as extended source ($5.2''$ aperture radius; dashed red line) and of the extended emission (in colour purple), obtained by subtracting the nuclear spectrum (solid green line) from the one extracted in the $5.2''$ aperture radius. All spectra have been smoothed.

Recovering nuclear information from low angular resolution data.

We used different methods to recover the nuclear emission of NGC 2992 from the low angular resolution data of Spitzer and Herschel. First, we performed spectral decomposition of the Spitzer/IRS spectrum using different SB templates and, 1) the MAP torus model shown in Fig. 3 or 2) the average torus models from Ramos Almeida et al. (2011; left and right panels of Fig. 5). Second, we tried to recover the nuclear IR SED using aperture photometry and Scaled PSF subtraction (see Fig. 6).

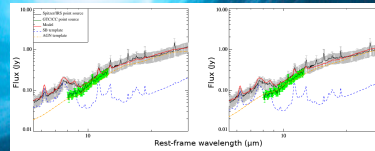


Fig. 5.- Spitzer/IRS decomposition in SB (blue line) and AGN (orange line) components.

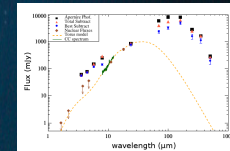


Fig. 6.- Nuclear IR SEDs of NGC 2992 from data of different angular resolutions.

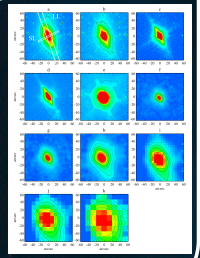


Fig. 7.- Spitzer and Herschel images of NGC 2992.

Physical parameters of the circumnuclear dust emission.

Dust grains are heated mainly by SF and nuclear activity, and this radiation is reemitted in the IR range. We fitted the circumnuclear and galaxy disk IR emission with modified blackbodies and we derived the dust temperatures, star formation rates (SFRs) and dust masses of the different components in the interacting system Arp 245. For the spiral galaxies, we find temperatures of ~ 30 K for the circumnuclear dust, typical of star-forming regions. On the other hand, the dust in the galaxy disk can be reproduced with a greybody of $T \sim 23$ K, characteristic of dust heated by the interstellar radiation field (see Fig. 8).

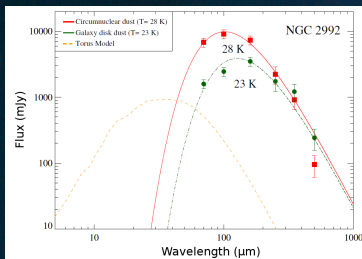


Fig. 8.- Greybody fits to the circumnuclear and galaxy disk dust (red and green lines respectively) and torus model shown in Fig. 3 (dashed orange line).

Name	Temperature (K)	SFR (M_\odot /yr)	M_{dust} ($10^6 M_\odot$)
NGC 2992 (Circumnuclear)	28 ± 2	2.3 ± 0.2	9.1 ± 0.9
NGC 2992 (Galaxy disk)	23 ± 1	0.80 ± 0.1	10.2 ± 1.1
NGC 2993 (Circumnuclear)	31 ± 3	3.0 ± 0.6	6.3 ± 1.2
NGC 2993 (Galaxy disk)	23 ± 1	0.8 ± 0.1	9.8 ± 0.9
Arp 245 North	17 ± 1	0.039 ± 0.003	3.1 ± 0.1
Arp 245 Bridge	19 ± 1	0.017 ± 0.002	0.7 ± 0.11

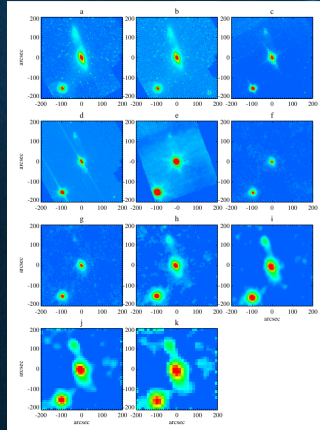


Fig. 9.- Spitzer and Herschel images of the Arp 245 system. NGC 2992 is the central galaxy, NGC 2993 is at the bottom left corner and Arp 245 North is at the top. All images have been smoothed. North is up, and east to the left.

Conclusions.

- The comparison between the GTC/CC spectrum of NGC 2992, which probes the central ~ 60 pc of the galaxy, and the Spitzer/IRS spectrum (~ 640 pc) reveals absent/suppressed PAH emission in central parsecs.
- We can reproduce the nuclear IR SED of NGC 2992 with a clumpy torus model of 1.2 pc radius and containing a mass of $M_{\text{torus}} = 9 \times 10^4 M_\odot$. The column density of the obscuring material is compatible with being Compton-thick, in agreement with X-ray observations (Weaver et al. 1996).
- Using low angular resolution photometry from Spitzer and Herschel, we can only recover the nuclear IR emission of NGC 2992 at 20 – 25 μ m, where the torus emission dominates.
- By decomposing the Spitzer/IRS spectrum in AGN and SB component, we can recover the nuclear information provided by the GTC/CC spectrum.
- From the spectral decomposition of the Spitzer/IRS spectrum we find that, whereas the SB component dominates the MIR emission at $\lambda \leq 15$ μ m, with 60 – 70% contribution at 6 μ m, the AGN component reaches 90% at 20 μ m.
- We reproduced the dust emission in the Arp 245 system using a set of modified blackbodies and derived similar SFRs and dust masses for the two spiral galaxies and significantly smaller for Arp 245 North, in agreement with Duc et al. (2000).

Ismael García-Bernet



References

- Duc P.-A., et al. 2000, AJ, 120, 1238
- Ramos Almeida C., et al. 2011, ApJ, 731, 92
- Weaver K. A., et al. 1996, ApJ, 458, 160

¹ *Bayesclumpy*: Asensio Ramos A. & Ramos Almeida C., 2009, ApJ, 696, 2075